

Grain orientation and electrical properties of $\text{Sr}_2\text{Nb}_2\text{O}_7$ ceramics

MIKIO FUKUHARA[†], CHI-YUEN HUANG, A. S. BHALLA, R. E. NEWNHAM
*Materials Research Laboratory, The Pennsylvania State University, University Park,
 Pennsylvania, 16802, USA*

$\text{Sr}_2\text{Nb}_2\text{O}_7$ ceramics sintered at 1753 K and the hot-pressed compacts annealed at 1073 K possess low density because of the formation of voids by large expansion. The expansion is attributed to cleavage and due to the preferential grain growth along the $\langle 010 \rangle$ direction. An increase in dielectric constant at temperatures over 973 K and a parabolic decrease of resistivity with increasing temperature are observed. The constant variation corresponds well to the decrease in thermal strain and the grain orientation factor along the $\langle 0k0 \rangle$ direction.

1. Introduction

Strontium niobate ($\text{Sr}_2\text{Nb}_2\text{O}_7$) is known to belong to the ferroelectric $\text{A}_2\text{B}_2\text{O}_7$ -type oxide compounds [1, 2]. Single crystals grown from the melt have remarkable piezoelectric and electro-optic properties [3, 4]. It has been reported that $\text{Sr}_2\text{Nb}_2\text{O}_7$ has two phase transitions [4], the first being ferroelectric phase transition at 1615 K with a dielectric anomaly along the c -axis, and the second a phase transition at 117 K with a dielectric anomaly along the b -axis. Ohi *et al.* [5] reported an additional phase transition at 488 K accompanied by changes in the elastic and dielectric properties. The atomic positions in $\text{Sr}_2\text{Nb}_2\text{O}_7$ at room temperature were determined by Ishizawa *et al.*, [6] with a change in symmetry from Cmcm to $\text{Cmc}2_1$ at the ferroelectric phase transition. Subsequent investigation by Yamamoto *et al.* [7, 8] with the electron microscope revealed that $\text{Sr}_2\text{Nb}_2\text{O}_7$ has an incommensurate phase, modulated with a wave vector $k = \pm (1/2 - \delta)a^* \pm c^*$ below about 488 K (where a^* and c^* are reciprocal lattice vectors) and an intricate domain-like texture. And they also discovered another structural phase transformation near 493 K in the ferroelectric phase. Based on studies of the numerous phase transitions and crystal morphology, it appears that the properties of $\text{Sr}_2\text{Nb}_2\text{O}_7$ depend on fabricating conditions, because the structures are composed of slabs with distorted perovskite-type octahedra stacked along the $[010]$ axis [6].

All the single crystals used in these works [2-8] were grown by the same floating-zone technique at high temperature near the melting point of 1973 K [4, 9, 10]. However, single crystals are impractical for most ferroelectric devices, because of the expense of obtaining high quality specimens. In this paper, polycrystalline $\text{Sr}_2\text{Nb}_2\text{O}_7$ ceramics are synthesized and their electrical properties are measured at high temperature, together with the lattice parameters. Of special interests are a large expansion of the sample

during sintering and/or annealing, and an understanding of the increase in dielectric constant and the decrease of resistivity at high temperatures.

2. Experimental procedure

The starting materials were SrCO_3 (Alfa Products, reagent) and Nb_2O_5 (Fansteel, HP-176). The powders were mixed in a 2:1 molar ratio, using a vibrating mill constructed of a plastic container and plastic balls in ethyl alcohol to prevent the contamination by other metals. The mixture was cold pressed at a pressure of about 127 MPa and calcined at 1273 K for 10.8 ksec in air. The calcined samples were then ground in an agate mortar and recalcined for 7.2 ksec at 1373 K in air. Although these powders contained a small amount of $\text{Sr}_5\text{Nb}_4\text{O}_{15}$ in addition to $\text{Sr}_2\text{Nb}_2\text{O}_7$, they were used as starting powders, because sintering temperatures below 1673 K were insufficient to achieve complete solid-state reaction [11]. They were cold pressed into discs 12.8 mm diameter at 245 MPa and then sintered at 1373 to 1873 K for 3.6 ksec in air. To densify the samples further, recalcined powders were hot pressed in argon at 1573 K for 3.6 ksec under a pressure of 1.97 MPa and then annealed at 1073 to 1873 K for 3.6 ksec in air. All samples were packed in recalcined powders during sintering in order to prevent contamination by the zirconia setter and furnace atmosphere. Quantitative analysis for the total impurities was carried out by a spectrographic emission technique (Jarrel-Ash Spectrograph). The results are presented in Table I.

X-ray diffraction measurements at room temperature were carried out with a SCINTAG PAD V diffractometer using $\text{CuK}\alpha$ radiation. A computer-controlled high-temperature X-ray diffractometer [12] was used to determine the lattice parameters from room temperature to 1273 K. Data collected by step-scanning around each peak were curve-fitted and

[†] Present address: Toshiba Tungaloy 1-7, Tsukagoshi, Saiwal-Ku, Kawasaki, 210 Japan.

TABLE I Spectrographic analysis (wt %) for impurities of a $\text{Sr}_2\text{Nb}_2\text{O}_7$ ceramic sintered at 1673 K

Ba	Ca	Al	Si	Mg	Fe	Ti	Not detected
0.05–0.2	0.05–0.2	0.01–0.05	0.01–0.05	< 0.01	< 0.01	< 0.01	B, Mn, Ni, Co, Cr, V, Sn, Bi, Pb, Zr, Be, Mo, Cu, Ag, Y

TABLE II Lattice parameters of $\text{Sr}_2\text{Nb}_2\text{O}_7$

Reference	a (nm)	b (nm)	c (nm)	V (nm ³)	Material
Present work	0.3956(7)	2.6784(5)	0.5703(3)	0.6044	Ceramics
Nanamatsu <i>et al.</i> [4]	0.397 ± 0.001	2.686 ± 0.005	0.572 ± 0.002	–	Single crystal
Ishizawa <i>et al.</i> [6]	0.3933(6)	2.6726(7)	0.5683(4)	0.5974	Single crystal
Smith and McCarthy [16]	0.3955(2)	2.678(2)	0.5701(2)	0.6038	Ceramic

precise peak positions (better than $0.01^\circ 2\theta$) were obtained. Consequently lattice parameters with standard deviations of two parts per 100 000 were obtained. Fractured surfaces of sintered samples were examined by a scanning electron microscope. To determine bulk thermal expansion coefficients and thermal strain, a rectangular bar ($0.5 \times 0.6 \times 2.1 \text{ cm}^3$) cut from the sintered sample, was used on Harrop Dilatometric Analyser; the instrument was first calibrated using a standard fused silica sample and the heating and cooling rates were adjusted to $8.3 \times 10^{-3} \text{ K sec}^{-1}$ in the programmer.

The dielectric measurements were carried out on an automated system in which a temperature control box (Model 2300, Delta Design Inc.) and LCR meter (Model 4274A, Hewlett Packard Inc.) were controlled by a desk-top computer system (Model 9816, Hewlett Packard Inc.). The capacitance, dielectric constant and resistivity were measured at 100, 200 and 400 Hz, 1, 2, 10, 20 and 100 kHz over the temperature range of room temperature to 1323 K during the heating run. Dielectric loss could not be obtained due to conductivity trouble at high temperature. As electrodes, both flat sides of the disc sample were coated with a thick platinum film using a d.c. sputtering apparatus and then annealed at 1273 K for 60 sec. Dielectric measurements were carried out on unpoled samples. The variation of polarization with electric field was measured at room temperature and at 50 Hz using a modified Sawyer and Tower circuit. Dimensions of the specimen were 8 mm diameter and 0.25 mm thick.

3. Results and discussion

3.1. Sinterability and grain orientation

The recalced powder compacts of $\text{Sr}_2\text{Nb}_2\text{O}_7$ were sintered in the temperature range 1373 to 1873 K. Theoretical density (%) of the sintered compounds is shown in Fig. 1, together with the grain orientation factor, f , along the $\langle 0k0 \rangle$ direction discussed later. With increasing temperature, the density shows a maximum value at 1753 K and unexpectedly decreases over 1773 K. Fractured surfaces of samples which show maximum density and large expansion, are presented in Fig. 2a and b, respectively. These samples are composed of flat layer-like grains having rectangular shape. In contrast with Fig. 2a, a large

number of pores can be found among grain boundaries in the microstructure of Fig. 2b as if the materials were wrenched open, prying the grains apart. Fine stripes are also observed in each grain of Fig. 2, and always in parallel to the length of each rectangular grain boundary [13]. Such a grain shape seems to be common to all the piezoelectric ceramics, and a pattern of fine stripes is similar to the case of perovskite-type ferroelectric ceramics [14] and may be associated with domain structure. An X-ray diffraction pattern of an as-sintered compact sintered at 1873 K is shown in Fig. 3. The XRD patterns of the samples sintered at higher temperature are characterized by intense $\{0k0\}$ reflections. The grains are found to be preferentially oriented with the b -axes and the orientation factor, f , can be estimated by comparing the X-ray diffraction patterns with those of unoriented ceramic calcined at 1273 K [15]. A ratio, p , of the sum of the intensities $I\{0k0\}$ of the $\{0k0\}$ reflections to the sum of the intensities $I\{hkl\}$ including $\{0k0\}$ is calculated using all lines between 10° and $55^\circ 2\theta$ listed in the JCPDS card, so f is defined as

$$f = (p - p_0)/(1 - p_0) \quad (1)$$

where p_0 is a value for an unoriented sample. p is calculated from

$$p = \frac{\sum_h I\{0k0\}}{\sum_{h,k,l} I\{hkl\}} \quad (2)$$

As shown in Fig. 1, the orientation factor f increases steeply with increasing temperature over 1673 K.

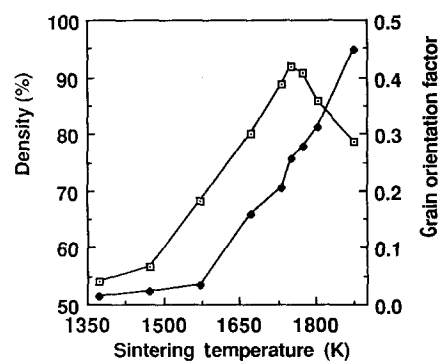


Figure 1 Dependence of (\square) density and (\blacklozenge) grain orientation factor along the $\langle 0k0 \rangle$ direction on sintering temperature.

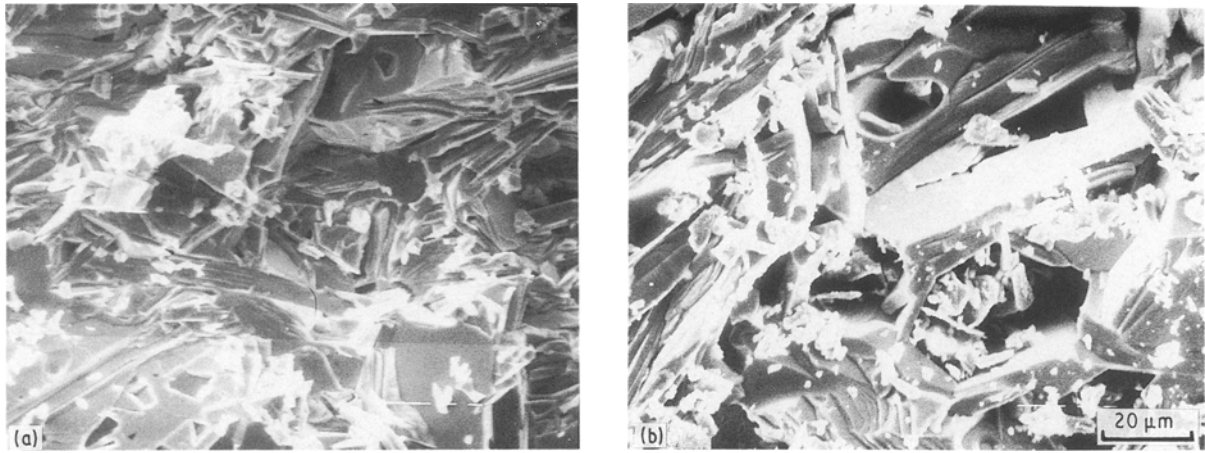


Figure 2 Photographs of fractured surfaces of sintered $\text{Sr}_2\text{Nb}_2\text{O}_7$ ceramics; (a) maximum density ceramic sintered at 1753 K, (b) maximum expanded ceramic sintered at 1873 K.

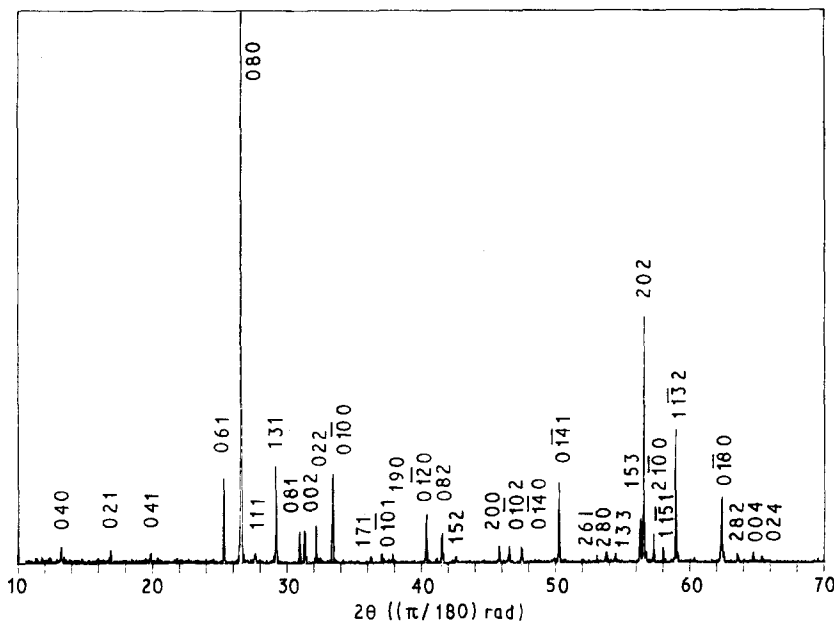


Figure 3 X-ray diffraction patterns for $\text{Sr}_2\text{Nb}_2\text{O}_7$ samples sintered at 1873 K.

Comparing the deterioration in the density over 1753 K with the orientation factor f , it appears that the grain orientation along the b -axis at elevated temperature hinders sinterability of $\text{Sr}_2\text{Nb}_2\text{O}_7$.

All the sintered samples are clearly indexed as a single phase within 2θ tolerance of 0.01° on the basis of an orthorhombic unit cell. The unit cell constants obtained at room temperature are given in Table II, together with the literature values. The lattice parameters obtained from ceramics data are almost the same, but are somewhat different from the single-crystal values, suggesting deviation from the stoichiometric composition of the two single crystals. Indeed, Carruthers and Graso [11] have reported that $\text{Sr}_2\text{Nb}_2\text{O}_7$ single crystals with stoichiometric composition could not be obtained.

Because we were unable to obtain samples with sintered densities over 92%, additional experiments were carried out by hot-pressing and annealing in air. The annealing treatment was required to remove small amounts of carbon in the hot-pressed samples. The effect of annealing temperature on density and the grain orientation factor along the $\langle 0k0 \rangle$ direction

was investigated in hot-pressed compacts with 98% theoretical density. As shown in Fig. 4, there is a rapid decrease in density for temperatures around 1073 K. The abrupt decrease in density corresponds closely to a change in preferred orientation along the b -axis in $\text{Sr}_2\text{Nb}_2\text{O}_7$. Because the crystal cleaves perfectly along the (010) plane [4], the preferential crystal growth

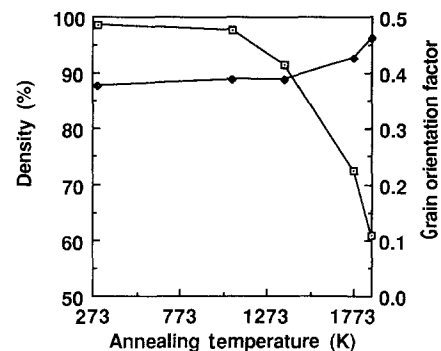


Figure 4 Dependence of (\square) density and (\blacklozenge) grain orientation factor along the $\langle 0k0 \rangle$ direction on annealing temperature for hot-pressed $\text{Sr}_2\text{Nb}_2\text{O}_7$ bodies.

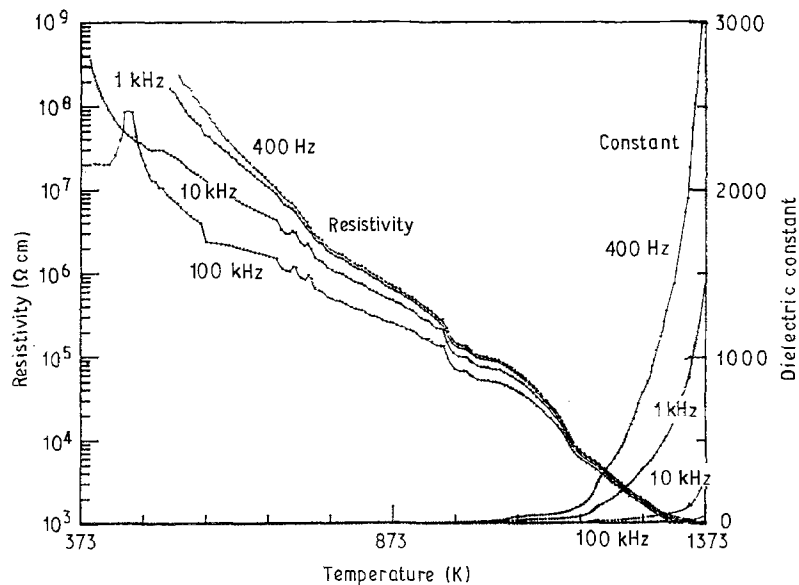


Figure 5 The temperature dependencies of dielectric constant and a.c. resistivity for hot-pressed $\text{Sr}_2\text{Nb}_2\text{O}_7$ ceramic annealed at 1073 K.

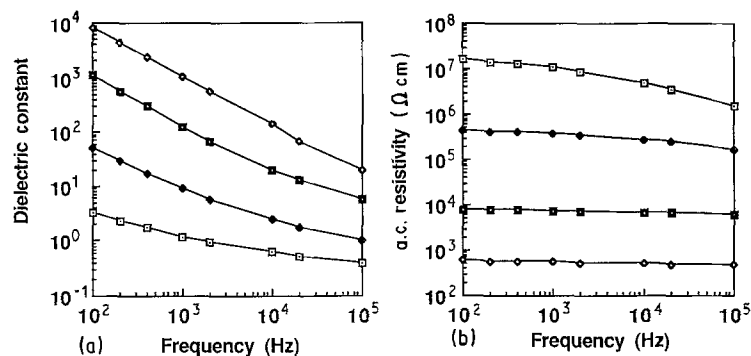


Figure 6 The frequency dependence of (a) dielectric constant and (b) a.c. resistivity on various temperatures for hot-pressed $\text{Sr}_2\text{Nb}_2\text{O}_7$ ceramic annealed at 1073 K. (□) 673 K, (◆) 923 K, (■) 1173 K, (◈) 1373 K.

along the $\langle 0k0 \rangle$ direction causes cleavage of the crystal and results in the formation of voids accompanied by expansion of the sample. To avoid electrode problems[†], the dielectric constant and electric resistivities were investigated using hot-pressed compacts, annealed at 1073 K, with 98% theoretical density.

3.2. Permittivity and electrical resistivity measurements

Dielectric constant and a.c. resistivity of hot-pressed $\text{Sr}_2\text{Nb}_2\text{O}_7$ ceramics were measured as a function of temperature by heating from room temperature to 1373 K. Representative plots of the dielectric constant and resistivity at various temperatures and frequencies are shown in Fig. 5. Measured K values at several frequencies show a steep increase around 1173 K and a parabolic decrease (semi-conducting behaviour) of resistivity without any noticeable change. The variation of the constant resembles that reported by Nanamatsu *et al.* [4] for polycrystalline samples. The dielectric anomalies at 488 and 493 K reported by Ohi *et al.* [5] and Yamamoto *et al.* [7, 8] were not observed in this study. It is not clear whether the increase of the constant arises from the ferroelectric transition

at 1615 K or due to the other causes, because of the limitations of our high-temperature measurement. From the data of the ceramics by Nanamatsu *et al.* [4], it is probably the former. Fig. 6a and b show the frequency dependence of the constant and the resistivity for various measuring temperatures, respectively. The constant considerably decreases independent of temperature with increasing frequency, but the resistivity decreases with frequency as the temperature increases and almost saturates at 1373 K. Although the increase in the constant at low frequency near room temperature generally arises from a space charge polarization at grain boundaries of ceramics [17], both types of behaviour (the simultaneous high constant and the low resistivity at high temperature) cannot be explained by this polarization mechanism. It requires further investigation.

$\text{Sr}_2\text{Nb}_2\text{O}_7$ ceramics used in this study contains a small amount of impurities (at least 0.17 mol % Ba, 0.58 mol % Ca, 0.17 mol % Al, 0.16 mol % Si, 0.19 mol % Mg, 0.08 mol % Fe and 0.09 mol % Ti), as can be seen from Table I. The question of whether these impurities influence a.c. conduction at elevated temperature in Fig. 5 cannot be answered at the present time. It is generally known that the effect on electric

[†] In a preliminary experiment, platinum coated on the porous sample showed abnormal rise in capacitance at around 1073 K.

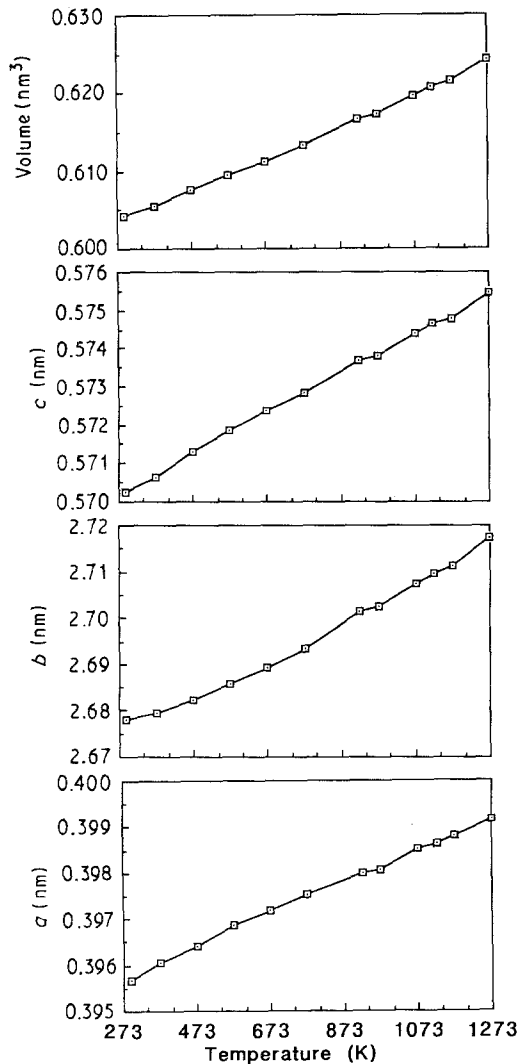


Figure 7 Thermal expansion of $\text{Sr}_2\text{Nb}_2\text{O}_7$ ceramic.

conductivity is remarkably high in the low-temperature region due to the structure sensitivity, but it disappears in the high-temperature one [18]. The influence on impurity in other results seems to be negligible within the impurity limit in the ferroelectric study [4] of $\text{Sr}_2\text{Nb}_2\text{O}_7$ -based solid solution with tantalum, calcium, lead and barium.

The definite polarization–electric field hysteresis loop for the ceramic could not be observed at room temperature, because of very high coercive field E_c [19]. Nor could the ceramics be poled with a d.c. applied voltage of 80 kV cm^{-1} in an oil bath at 473 K, or at 450 kV cm^{-1} in corona poling at 445 K.

3.3. High-temperature measurement of lattice dimension

In order to investigate the high-temperature properties of $\text{Sr}_2\text{Nb}_2\text{O}_7$, the lattice parameters and thermal expansion coefficients were measured from room temperature to about 1300 K. The results are presented in Figs 7 and 8, respectively. Neither figure shows a distinct change in the temperature range 293 to 1273 K, but the contraction curve observed on the cooling run of Fig. 8 shows a small inflection at around 1300 K. Coefficients of thermal expansion

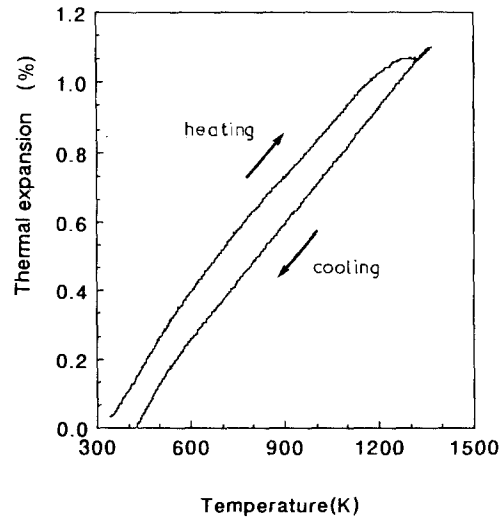


Figure 8 Lattice parameters of $\text{Sr}_2\text{Nb}_2\text{O}_7$ plotted against temperature.

calculated from Fig. 7 are $\alpha_a = 9.0 \times 10^{-6}$, $\alpha_b = 14.9 \times 10^{-6}$, $\alpha_c = 9.2 \times 10^{-6} \text{ K}^{-1}$ and that from Fig. 8 is $10 \times 10^{-6} \text{ K}^{-1}$. The small negative deviation from the straight line in the thermal expansion during heating run of Fig. 8 is about twice the expansion of the b -axis compared with those of a - or c -axes. Such a thermal expansion anisotropy could be responsible for the occurrence of fracture in highly anisotropic $\text{Sr}_2\text{Nb}_2\text{O}_7$ ceramics.

Because thermally-induced fracture clearly depends on large grain size [20], the control of grain size is a major problem in the polycrystalline $\text{Sr}_2\text{Nb}_2\text{O}_7$ ceramics. The thermal strain was calculated from the expansion curve in Fig. 8. This result is shown in Fig. 9. The strain begins to decrease from around 1000 K, and shows a negative maximum value at around 1305 K. Over that temperature the strain again increases with increasing temperature. Thus, it is concluded that the grain growth during sintering and hot pressing causes the $\{0k0\}$ plane cleavage of the crystal under large internal stresses and results in accumulation of the mechanical strain at the crystal grain boundaries. Fig. 10 shows temperature dependence of the grain orientation factor along the $\langle 0k0 \rangle$ direction, where the factor begins to decrease from around 973 K where the dielectric constant begins to increase. Because the intensities in normal metals decrease smoothly as the temperature of the crystal increases

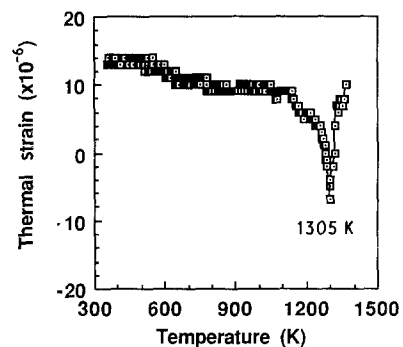


Figure 9 The temperature dependence of thermal strain of $\text{Sr}_2\text{Nb}_2\text{O}_7$ ceramic.

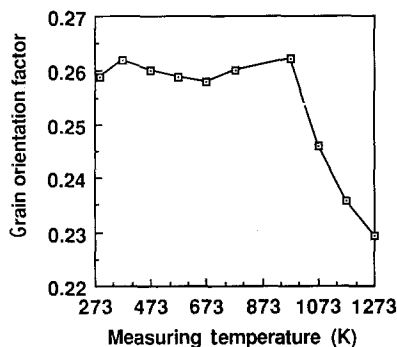


Figure 10 The temperature dependence of the grain orientation factor along the $\langle 0k0 \rangle$ direction in $\text{Sr}_2\text{Nb}_2\text{O}_7$ ceramic.

[21, 22], the inflection would be related to the relief of strain and the increment of the constant. Indeed, it has been known that the residual strain deteriorates the permittivity and lowers the Curie points of ferroelectric compounds such as BaTiO_3 and $\text{Ba}(\text{Ti}, \text{Sn})\text{O}_3$ [23].

4. Conclusion

Polycrystalline $\text{Sr}_2\text{Nb}_2\text{O}_7$ ceramics were synthesized and their electrical properties and high-temperature lattice dimension were investigated. The following conclusions are drawn.

1. The density reaches a maximum value when the samples are sintered at 1753 K, and higher temperatures induce a large expansion of the sample due to the formation of voids. The hot-pressed sample also shows expansion after annealing. The expansion is perhaps attributable to cleavage of the crystal which is caused by preferential grain growth along the $\langle 0k0 \rangle$ direction.

2. An increase in the dielectric constant over 973 K and a parabolic decrease of a.c. resistivity with increasing temperature are observed. The increment in the constant corresponds well to the decrease of the thermal strain and the grain orientation factor.

Acknowledgements

We thank Dr Q. C. Xu and A. Ando for useful discussions.

References

- G. A. SMOLENSKI, V. A. ISUPOV and A. I. AGRANOVSKAIA, *Sov. Phys. Dokl.*, **1** (1956) 300.
- W. KINASE, S. NANAMATSU, N. ISHIHARA, K. HASEGAWA and K. YANO, *Ferroelectrics* **38** (1981) 849.
- S. NANAMATSU, M. KIMURA, K. DOI and M. TAKAHASHI, *J. Phys. Soc. Jpn* **30** (1971) 300.
- S. NANAMATSU, M. KIMURA, T. KAWAMURA, *ibid.* **38** (1975) 817.
- K. OHI, M. KIMURA, H. ISHIDA and KAKIMURA, *ibid.* **46** (1979) 1387.
- N. ISHIZAWA, F. MARUMO, T. KAWAMURA and M. KIMURA, *Acta Crystallogr.* **B31** (1975) 1912.
- N. YAMAMOTO, K. YAGI, G. HONJO, M. KIMURA and T. KAWAMURA, *J. Phys. Soc. Jpn* **48** (1980) 185.
- N. YAMAMOTO, *Acta Crystallogr.* **A38** (1982) 789.
- T. AKASHI, K. MATSUI, T. OKADA and T. MIZUTANI, *IEEE Trans. Mag.* **Mag-5** (1969) 285.
- M. TAKAHASHI, S. NANAMATSU and M. KIMURA, *J. Crystal Growth* **13/14** (1972) 68.
- J. R. CARRUTHERS and M. GRASO, *J. Electrochem. Soc. Solid State Sci.* **17** (1970) 1426.
- G. E. LENAIN, H. A. MCKINSTRY and S. Y. LIMAYE, "Advances in X-Ray Analysis", Vol. 28, edited by C. S. Barret, Greacchi and Leyder (Plenum, New York, 1985) p. 345.
- S. IKEGAMI and I. UEDA, *Jpn. J. Appl. Phys.* **13** (1974) 1572.
- R. C. DeVRIES and J. E. BURKE, *J. Amer. Ceram. Soc.* **40** (1957) 200.
- F. K. LOTGERING, *J. Inorg. Nucl. Chem.* **9** (1959) 113.
- C. SMITH and G. J. McCARTHY, Pennsylvania State University, 1976 (JCPDS, 1978) **28-1245**.
- K. OKAZAKI, "Ceramic Engineering for Dielectrics", 3rd Edn (Gakken-Sha, Tokyo, 1983) p. 307.
- Y. INUISHI, T. NAKAJIMA, K. KAWABE and M. IEDA, "Dielectric Behaviors", 15th Edn (Japan Electric Society, Tokyo, 1986) pp. 208, 221.
- S. NANAMATSU and M. KIMURA, *J. Phys. Soc. Jpn.* **36** (1974) 1495.
- R. W. RICE and R. C. POHANKA, *J. Amer. Ceram. Soc.* **62** (1979) 559.
- R. M. NICKLOW and R. A. YOUNG, *Phys. Rev.* **152** (1966) 591.
- C. KITTEL, "Introduction to Solid State Physics", 6th Edn (Wiley, New York, 1988) p. 603.
- K. OKAZAKI and S. KASHIWABARA, *J. Ceram. Assoc. Jpn* **73** (1965) 60.

Received 30 October 1989
and accepted 21 November 1989